

Nanofocusing of light using three-dimensional plasmonic mode conversion

Shinmo An,¹ Hyun-Shik Lee,¹ Yong-Beom Jeong,¹ Young Chul Jun,² Seung Gol Lee,¹ Se-Guen Park,¹ El-Hang Lee,¹ and O. Beom-Hoan^{1,*}

¹LED-Smart Technology Advanced Research (LED-STAR) Center, Micro/Nano-Photonics Advanced Research Center (m-PARC), Department of Electronic Engineering, Inha University, Incheon 402-751, South Korea

²LED-Smart Technology Advanced Research (LED-STAR) Center, Department of Physics, Inha University, Incheon 402-751, South Korea

*obh@inha.ac.kr

Abstract: Efficient nanofocusing of light into a gap plasmon waveguide using three-dimensional mode conversion in a strip plasmonic directional coupler is proposed. Unlike conventional nanofocusing using tapering structures, a plasmonic directional coupler converts E_z -type odd mode energy into E_y -type gap plasmon mode by controlling phase mismatch and gap spacing. The simulation result shows the maximum electric field intensity increases up to 58.1 times the input intensity, and 17.3% of the light is focused on the nano gap region.

©2013 Optical Society of America

OCIS codes: (240.6680) Surface plasmons; (260.5950) Self-focusing.

References and links

1. K. Okamoto, I. Niki, A. Shvartser, Y. Narukawa, T. Mukai, and A. Scherer, "Surface-plasmon-enhanced light emitters based on InGaN quantum wells," *Nat. Mater.* **3**(9), 601–605 (2004).
2. R. F. Oulton, V. J. Sorger, T. Zentgraf, R. M. Ma, C. Gladden, L. Dai, G. Bartal, and X. Zhang, "Plasmon lasers at deep subwavelength scale," *Nature* **461**(7264), 629–632 (2009).
3. A. V. Akimov, A. Mukherjee, C. L. Yu, D. E. Chang, A. S. Zibrov, P. R. Hemmer, H. Park, and M. D. Lukin, "Generation of single optical plasmons in metallic nanowires coupled to quantum dots," *Nature* **450**(7168), 402–406 (2007).
4. P. Neutens, P. Van Dorpe, I. De Vlaminck, L. Lagae, and G. Borghs, "Electrical detection of confined gap plasmons in metal-insulator-metal waveguides," *Nat. Photonics* **3**(5), 283–286 (2009).
5. H. Ditlbacher, A. Hohenau, D. Wagner, U. Kreibitz, M. Rogers, F. Hofer, F. R. Aussenegg, and J. R. Krenn, "Silver nanowires as surface plasmon resonators," *Phys. Rev. Lett.* **95**(25), 257403 (2005).
6. D. K. Gramotnev and S. I. Bozhevolnyi, "Plasmonics beyond the diffraction limit," *Nat. Photonics* **4**(2), 83–91 (2010).
7. P. Berini, "Air gaps in metal stripe waveguides supporting long-range surface plasmon polaritons," *J. Appl. Phys.* **102**(3), 033112 (2007).
8. Y. H. Joo, M. J. Jung, J. Yoon, S. H. Song, H. S. Won, S. Park, and J. J. Ju, "Long-range surface plasmon polaritons on asymmetric double-electrode structures," *Appl. Phys. Lett.* **92**(16), 161103 (2008).
9. A. Hosseini, H. Nejati, and Y. Massoud, "Design of a maximally flat optical low pass filter using plasmonic nanostrip waveguides," *Opt. Express* **15**(23), 15280–15286 (2007).
10. H. Lee, J. Song, and E. Lee, "An effective excitation of the lightwaves in the plasmonic nanostrip by way of directional coupling," *J. Korean Phys. Soc.* **57**(61), 1577–1580 (2010).
11. J. Song, H. Lee, B. O. S. Lee, S. Park, and E. Lee, "Design of nanoring resonators made of metal-insulator-metal nanostrip waveguides," *J. Korean Phys. Soc.* **57**(61), 1789–1793 (2010).
12. D. F. P. Pile, D. K. Gramotnev, M. Haraguchi, T. Okamoto, and M. Fukui, "Numerical analysis of coupled wedge plasmons in a structure of two metal wedges separated by a gap," *J. Appl. Phys.* **100**(1), 013101 (2006).
13. G. Veronis and S. Fan, "Guided subwavelength plasmonic mode supported by a slot in a thin metal film," *Opt. Lett.* **30**(24), 3359–3361 (2005).
14. G. B. Hoffman and R. M. Reano, "Vertical coupling between gap plasmon waveguides," *Opt. Express* **16**(17), 12677–12687 (2008).
15. B. Wang and G. P. Wang, "Surface plasmon polariton propagation in nanoscale metal gap waveguides," *Opt. Lett.* **29**(17), 1992–1994 (2004).
16. P. Ginzburg, D. Arbel, and M. Orenstein, "Gap plasmon polariton structure for very efficient microscale-to-nanoscale interfacing," *Opt. Lett.* **31**(22), 3288–3290 (2006).
17. H. Choi, D. F. P. Pile, S. Nam, G. Bartal, and X. Zhang, "Compressing surface plasmons for nano-scale optical

- focusing,” *Opt. Express* **17**(9), 7519–7524 (2009).
18. V. S. Volkov, S. I. Bozhevolnyi, S. G. Rodrigo, L. Martín-Moreno, F. J. García-Vidal, E. Devaux, and T. W. Ebbesen, “Nanofocusing with Channel Plasmon Polaritons,” *Nano Lett.* **9**(3), 1278–1282 (2009).
 19. S. Vedantam, H. Lee, J. Tang, J. Conway, M. Staffaroni, and E. Yablonovitch, “A plasmonic Dimple Lens for Nanoscale Focusing of Light,” *Nano Lett.* **9**(10), 3447–3452 (2009).
 20. E. Verhagen, L. K. Kuipers, and A. Polman, “Plasmonic Nanofocusing in a Dielectric Wedge,” *Nano Lett.* **10**(9), 3665–3669 (2010).
 21. S. I. Bozhevolnyi and K. V. Nerkararyan, “Adiabatic nanofocusing of channel plasmon polaritons,” *Opt. Lett.* **35**(4), 541–543 (2010).
 22. M. Schnell, P. Alonso-Gonzalez, L. Arzubiaga, F. Casanova, L. E. Hueso, A. Chuvilin, and R. Hillenbrand, “Nanofocusing of mid-infrared energy with tapered transmission lines,” *Nat. Photonics* **5**(5), 283–287 (2011).
 23. M. I. Stockman, “Erratum: Nanofocusing of Optical Energy in Tapered Plasmonic Waveguides [*Phys. Rev. Lett.* **93**, 137404 (2004)],” *Phys. Rev. Lett.* **106**, 019901 (2011).
 24. H. Choo, M. Kim, M. Staffaroni, T. J. Seok, J. Bokor, S. Cabrini, P. J. Schuck, M. C. Wu, and E. Yablonovitch, “Nanofocusing in a metal-insulator-metal gap plasmon waveguide with a three-dimensional linear taper,” *Nat. Photonics* **6**(12), 838–843 (2012).
 25. D. Marcuse, *Theory of Dielectric Optical Waveguides* (Academic, 1991, Vol. 2).
 26. J. Dionne, L. Sweatlock, H. Atwater, and A. Polman, “Planar metal plasmon waveguides: frequency-dependent dispersion, propagation, localization, and loss beyond the free electron model,” *Phys. Rev. B* **72**(7), 075405 (2005).
 27. S. Park, J. J. Ju, J. T. Kim, M. S. Kim, S. K. Park, J. M. Lee, W. J. Lee, and M. H. Lee, “Sub-dB/cm propagation loss in silver stripe waveguides,” *Opt. Express* **17**(2), 697–702 (2009).
-

1. Introduction

Focusing light at nano-scale size is an indispensable element for investigation and utilization of nano-scale optical/photonic devices, such as on-chip light-emitting diodes, lasers, quantum dots, detectors, and filters [1–5]. Surface plasmon polaritons (SPPs) have been suggested as a means of converging light below the diffraction limit of conventional focusing devices [6]. Existing on the metal-dielectric interface, SPPs have various structures [7–15]. Among them, the gap plasmon structures, also known as metal-insulator-metal (MIM) plasmons, have the possibility of light localization far beyond the diffraction limit because light is strongly localized in the dielectric layer between two parallel metal layers. The fundamental mode of the gap plasmon is symmetric four corner wedge plasmons that do not have cut-off separation [12,13]. This means the gap plasmon can be shrunk without dimensional limitations, so the gap plasmon has been favorably adopted in nanofocusing SPP structures. One of the critical problems in the gap plasmon, however, is its extremely low efficiency in light coupling from many orders of larger micro-scale light sources due to huge mode field size and wavevector differences. To solve these problems, efficient nanofocusing studies have been reported [16–24].

In this paper, we propose a three-dimensional nanofocusing structure based on strip surface plasmon waveguides consisting of a directional coupler. The directional coupler is a pair of waveguides placed in parallel, and a launched light in one waveguide transfers to the other waveguide with a period of transfer length [25]. A strip surface plasmon waveguide is a type of metal strip line with a bottom infinite metal plane and a dielectric spacing between two metal layers [9]. The mode field size and the effective index (wavevector) of the strip surface plasmon waveguide match well to that of the silicon waveguide. It has already been proven that light can be coupled efficiently into a strip plasmon waveguide from a silicon waveguide by indirect evanescent wave coupling instead of the bulk objective lens system [10]. We show in simulation that the launched longitudinally polarized fundamental mode of each strip plasmon waveguide in the directional coupler converges at the gap region between two metal strips in a horizontally polarized gap plasmon mode by matching the odd mode phase condition and gradual decreasing the gap spacing. This mode conversion effect is unusual in conventional dielectric material systems and happens only in metal-dielectric interface plasmonic devices.

2. Gap plasmon generation principle

Figure 1 shows a schematic diagram of the proposed nanofocusing scheme using the strip surface plasmonic directional coupler. The coupler consists of three regions denoted as (a) – a single strip plasmon waveguide, (b) – a double strip plasmonic directional coupler, and (c) – a gap plasmon waveguide. The sequence of the nanofocusing process is as follows. First, a longitudinally polarized (E_z -polarized) light is launched into the separated singlemode strip plasmon waveguides (A and A') with a 180° (π) phase difference. The left inset in Fig. 1 shows the cross-sectional view of the strip plasmon waveguide. The thickness of the metal strip (t_m) is 10 nm, and the width (w) is 200 nm. The dielectric layer thickness (t_d) between the metal strip and the bottom metal plate is 80 nm, and the area of the bottom metal plate is assumed to be infinite [9]. Because the dielectric layer thickness (t_d) is relatively thicker than the metal strip, the waveguide configuration can be viewed as an insulator-metal-insulator (IMI) structure. The separated waveguides converge to become a directional coupler at B. In a conventional directional coupler, when light is launched into one waveguide a mode transition occurs. This mode transition can be explained by coupled mode theory, which describes it with the combination of even and odd modes in two waveguides. If one of the even and odd modes is launched into the waveguides, the mode transition does not occur owing to the lack of the counterpart mode. In a nanofocusing plasmonic directional coupler, light is launched

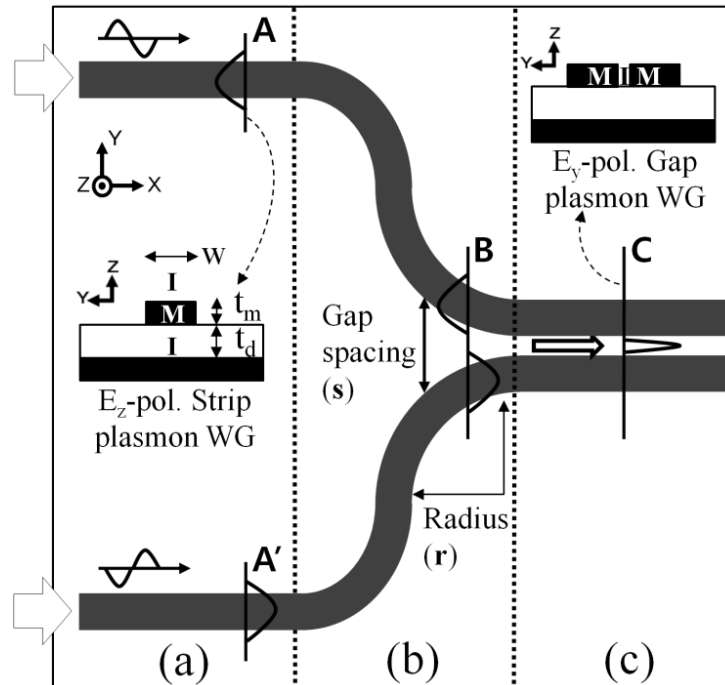


Fig. 1. Schematic diagram of the gap plasmon generation method using a strip plasmon directional coupler. Longitudinally polarized (E_z -pol.) plasmon mode is launched at the separate strip plasmon waveguides with a 180° -phase difference (A and A') in (a). The launched plasmon modes behave as an odd mode of the directional coupler B as the gap spacing decreases in (b). It converges at the gap region with a polarization change (E_y -pol.) with further decreasing of the gap spacing. Finally, the odd mode becomes a horizontally polarized gap plasmon mode C in (c).

into two waveguides with a 180° phase difference. Therefore, the light forms an odd mode in the directional coupler at B in Fig. 1(b) and it propagates without the mode transition. Finally, when the spacing between two strip plasmon waveguides (s) becomes even closer, the

longitudinally polarized electric field (E_z -polarized) converges at the gap region in the form of a horizontally polarized gap plasmon mode (E_y -polarized) at C in Fig. 1(c). Spacing (s) between the two metal strips gradually decreases to 5 nm along the directional coupler.

3. Effective index similarity between the plasmonic directional coupler and gap plasmon mode

The mode conversion phenomenon in the directional coupler can be explained by the effective index similarity between the odd mode of the strip plasmonic directional coupler and the gap plasmon mode. The effective index of the directional coupler depends on the gap spacing. We investigated the mode field characteristics of the strip plasmonic directional coupler using a finite element method (FEM) to clarify the relationship between effective index similarity and mode field distribution. Silver (Ag) is used as the metal. The permittivity of Ag is set to $-116.8 + i11.68$, and the corresponding refractive index is $0.5396 + i10.823$ at a $1.55 \mu\text{m}$ optical communication wavelength. The refractive index of the dielectric material is 1.45. We assumed that the dielectric material covers the metal strips.

Figure 2 shows the dependence of the real part of the effective index of the directional coupler on gap spacing (s). The insets show the waveguide configurations for the single strip plasmon waveguide A, the double strip plasmonic directional coupler B, and a reference gap plasmon waveguide in a metal slab, C'. For the single strip plasmon waveguide A, the real part of the effective index is 2.45524 with a 10 nm strip thickness (t_m), a 200 nm strip width (w), and an 80 nm dielectric thickness (t_d). The effective index of the strip plasmonic directional coupler B is similar to that of the single strip plasmon waveguide A when gap spacing is around 300 nm. As gap spacing decreases, the effective index of the strip plasmonic directional coupler diverges to even and odd modes. There is a crossing point of the effective indices of the even

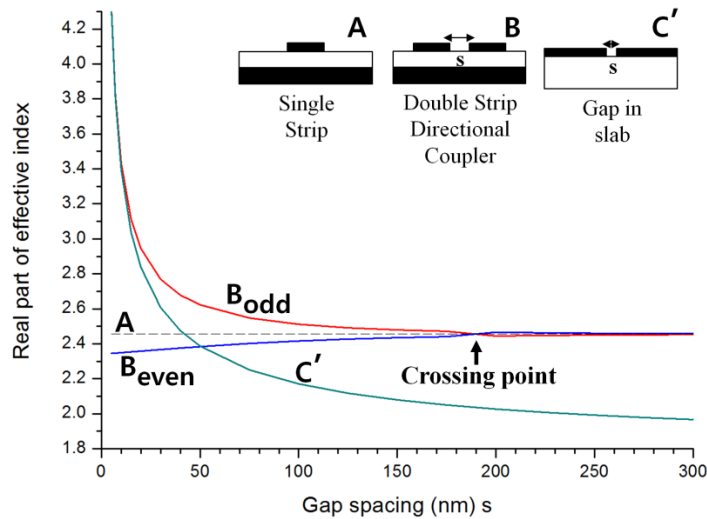


Fig. 2. Dependence of the real part of the effective indices of the strip plasmon directional coupler and the gap plasmon waveguide on gap spacing. The Fig. 2 shows the effective index of a single strip plasmon waveguide A, a double strip directional coupler for odd and even modes (B_{odd} and B_{even}), and a gap plasmon waveguide in a metal slab (C'). As gap spacing decreases, the effective index of the odd mode and gap plasmon mode increase and become similar.

and odd modes at around 190 nm gap spacing, called the infinite coupling length [11]. Below 190 nm, the effective index of the even mode starts to decrease gradually, whereas the effective index of the odd mode increases exponentially. The exponential increase of the odd mode B_{odd} is similar to the increase of the gap plasmon mode C' below 25 nm of gap

spacing. This similarity in the effective index between the odd mode of the strip plasmonic directional coupler and the gap plasmon mode means a possibility of energy transfer between them.

However, the fundamental mode of the strip plasmonic directional coupler is longitudinally polarized (E_z -polarized) which differs from the horizontally polarized (E_y -polarized) gap plasmon mode. There should be a continuous polarization transition between the strip plasmon mode and the gap plasmon in the directional coupler. We investigated the polarization characteristics of the directional coupler with respect to the gap spacing variance.

4. Polarization characteristics of the plasmonic directional coupler

Figure 3 shows a ratio variance of the E_y -field in the total power of the strip plasmon odd mode in the directional coupler with respect to gap spacing (s) and metal thickness (t_m). The E_y -field ratio in total power is calculated using the following formula:

$$E_{yfrac} = \frac{\int_{-\infty}^{\infty} (E_y H_z) ds}{\int_{-\infty}^{\infty} P_x(s) ds} \quad (1)$$

where, E_y is the horizontal electric field intensity, H_z is the longitudinal magnetic field intensity, P_x is Poynting power, and s is surface area.

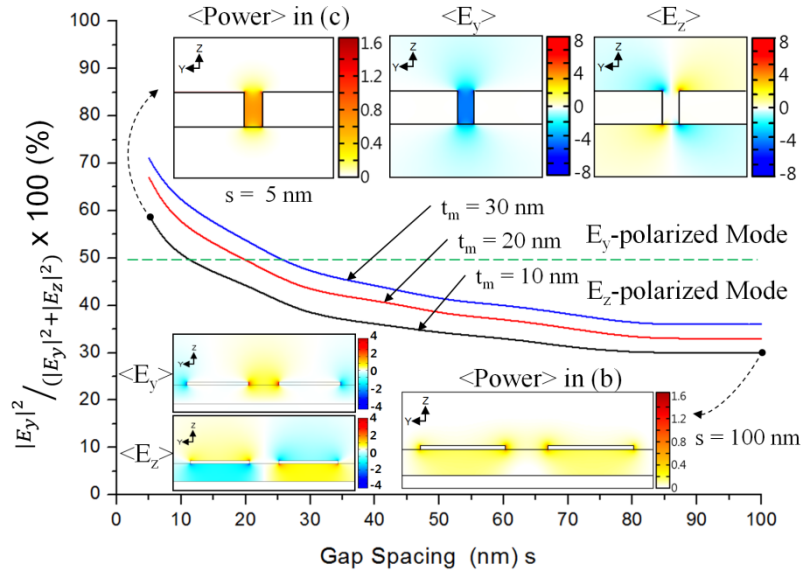


Fig. 3. Ratio variance of E_y -field in total power of the strip plasmon odd mode in the directional coupler with respect to gap spacing (s) and metal thickness (t_m). The bottom insets show a cross-sectional view of light power-, E_y - and E_z -fields distributions at gap spacing of 100 nm in (b). Light power distribution follows the E_z -field. As gap spacing decreases, the E_y -field ratio exceeds the E_z -field in total power. The top inset shows power, E_y - and E_z -fields distributions at gap spacing of 5 nm in (c). The increased power ratio of the E_y -field converges at the gap region. The power distribution follows the E_y -field rather than the E_z -field.

With gap spacing of 100 nm and metal thickness of 10 nm, the E_y -field ratio is around 30 percent. As gap spacing decreases, the E_y -field ratio increases. With gap spacing of 5 nm, the E_y -field ratio reaches 58 percent total power. Figure 3 show the cross-sectional view of the odd mode power distribution with gap spacing of 100 nm and 5 nm, which correspond to Figs. 1(b) and 1(c), respectively. With gap spacing of 100 nm, odd mode power is distributed like a conventional strip plasmon waveguide. Bottom left side inset Figs. show the cross-sectional view of the odd mode with E_y -field $\langle E_y \rangle$ and E_z -field $\langle E_z \rangle$ distributions. The power

distribution is likely to follow $\langle E_z \rangle$ distribution, which oscillates in a longitudinal direction. With gap spacing of 5 nm, however, the odd mode power distribution is concentrated at the gap region. When comparing with the inset electric field distributions of the E_y -field $\langle E_y \rangle$ and the E_z -field $\langle E_z \rangle$, we see similarity to the horizontal $\langle E_y \rangle$ distribution rather than the longitudinal $\langle E_z \rangle$ distribution.

Considering that the horizontal E_y -field ratio with total power exceeds 50 percent, and the mode power distribution of the directional coupler shows similarity to the $\langle E_y \rangle$ distribution, the odd mode in the surface plasmonic directional coupler with 5 nm spacing can be viewed as a longitudinally polarized (E_y) mode. Also, the continuously varying E_y -field ratio with total power in Fig. 3 means a mode conversion phenomenon happens in the directional coupler as gap spacing changes. By using this principle, we can focus the light into the deep sub-wavelength gap regions.

5. Simulation of the gap plasmon focusing

We verified this focusing mechanism using a commercial three-dimensional finite-difference time-domain (FDTD) simulation. We set the simulation time as 75 fs, time step as 0.00249634 fs and the dimension of the space grid as 5 nm, 1 nm, and 2 nm for X, Y, Z coordinates. In a simulation study, we launched the fundamental strip plasmon mode at both waveguides with a 180° phase difference A and A' in Fig. 1 to form the odd mode in the directional coupler B in Fig. 1. Here, the radius of curvature (r) in the directional coupler should be optimized to minimize the device size and total device absorption loss. Figure 4 shows the focused power percentage the gap region as a function of the x coordinate of the straight gap plasmon waveguide region (c) for radius (r) of the directional coupler. The radius is set to 150, 250, 350, and 450 nm, and the total propagation length is normalized to be equal. A power measuring monitor in our simulation is a square region with width and height of 60 nm x 60 nm. It is placed at the center of the gap region along the propagation axis with a period of 25 nm, and measures the focused light in the gap region. The focused power increases as the launched strip plasmon mode at A and A' propagates through the directional coupler in Fig. 4(b) and reaches maximum in the straight gap, Fig. 4(c), decreasing due to the absorption loss. The inset top left shows the cross-sectional view of the strip plasmon power distribution in the directional coupler with a gap spacing of 100 nm for Fig. 4(b), and the inset top right shows the focused gap plasmon power distribution with gap spacing of 5 nm for Fig. 4(c), which is transformed from the strip plasmon mode by the mode conversion phenomenon via the directional coupler. The result shows no noticeable difference in the radius of curvatures for 250, 350, and 450 nm, except for 150 nm because of the normalized total propagation length. The 150 nm radius shows relatively low focusing efficiency due to excessive bending loss in the curved region. We chose a radius of 450 nm, and the resulting focused power percentage at the gap region is 5.18%, 5.97%, 10.19%, and 17.3% for monitor windows of 5 nm x 10 nm, 10 nm x 10 nm, 20 nm x 20 nm, and 60 nm x 60 nm, respectively, including absorption and bending losses, with a total propagation length of 1500 nm. The focused gap plasmon mode shows an electric field intensity increment 58.1 times the initially launched strip plasmon mode.

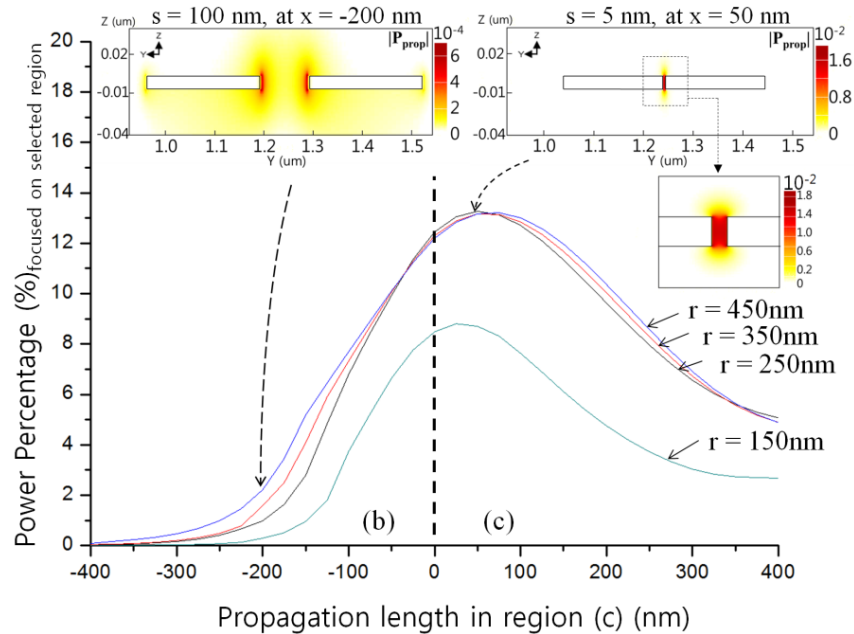


Fig. 4. Focused power percentage at the gap region as a function of the propagation length of the straight gap plasmon waveguide region (c) for radius (r) of the directional coupler. The focused power starts to increase in (b) and reaches the maximum in (c), decreasing due to absorption loss. The insets show cross-sectional power distribution of the directional coupler with spacings of 100 nm and 5 nm.

width and height of 60 nm x 60 nm. It is placed at the center of the gap region along the propagation axis with a period of 25 nm, and measures the focused light in the gap region. The focused power increases as the launched strip plasmon mode at A and A' propagates through the directional coupler in Fig. 4(b) and reaches maximum in the straight gap, Fig. 4(c), decreasing due to the absorption loss. The inset top left shows the cross-sectional view of the strip plasmon power distribution in the directional coupler with a gap spacing of 100 nm for Fig. 4(b), and the inset top right shows the focused gap plasmon power distribution with gap spacing of 5 nm for Fig. 4(c), which is transformed from the strip plasmon mode by the mode conversion phenomenon via the directional coupler. The result shows no noticeable difference in the radius of curvatures for 250, 350, and 450 nm, except for 150 nm because of the normalized total propagation length. The 150 nm radius shows relatively low focusing efficiency due to excessive bending loss in the curved region. We chose a radius of 450 nm, and the resulting focused power percentage at the gap region is 5.18%, 5.97%, 10.19%, and 17.3% for monitor windows of 5 nm x 10 nm, 10 nm x 10 nm, 20 nm x 20 nm, and 60 nm x 60 nm, respectively, including absorption and bending losses, with a total propagation length of 1500 nm. The focused gap plasmon mode shows an electric field intensity increment 58.1 times the initially launched strip plasmon mode.

When the launched fundamental strip plasmon mode in both waveguides is not at a 180° phase difference, the focused gap plasmon power deteriorates. Figure 5 shows the longitudinal electric field intensity ($|E_z|^2$) distribution of the strip plasmonic directional coupler for gap plasmon focusing, with an odd mode launching condition at a 180° phase difference Fig. 5(a) and an even mode launching condition at no phase difference Fig. 5(b). It intersects the middle of the Ag metal strip layer. In Fig. 5(a), the launched longitudinal electric field intensity distribution is concentrated on the out-curved side of the bended directional coupler. It finally disappears at the end of the curved directional coupler region. This means the

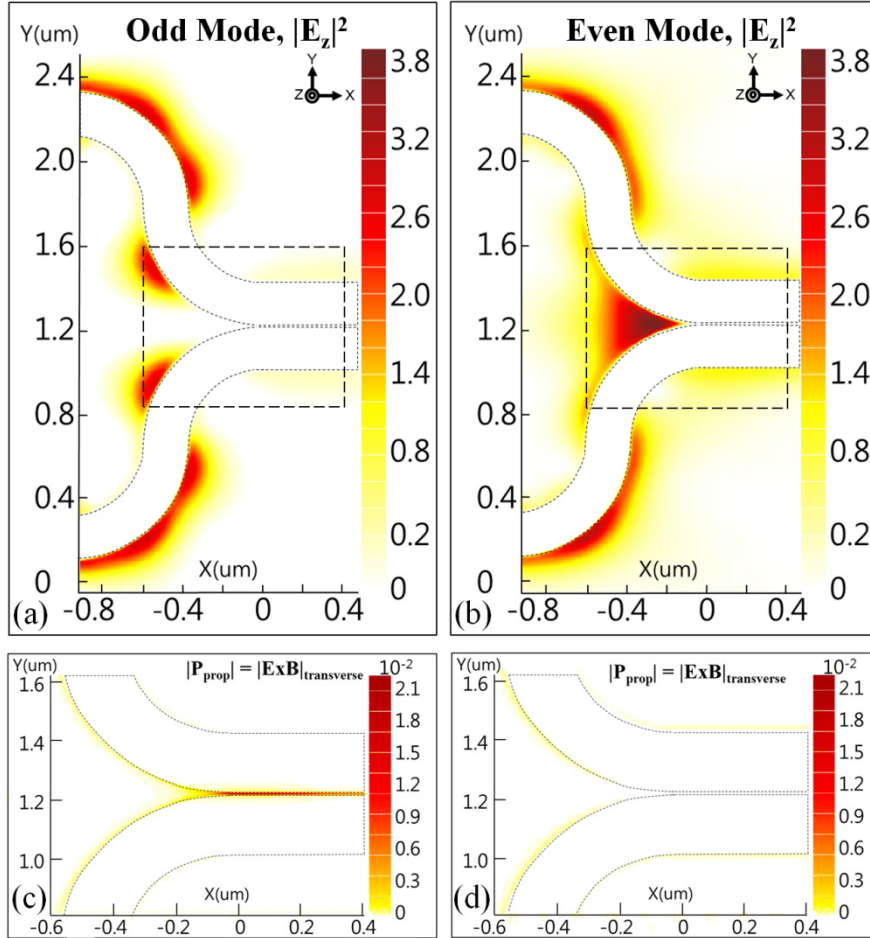


Fig. 5. Longitudinal electric field intensity ($|E_z|^2$) distribution of the strip plasmon directional coupler for the gap plasmon focusing with (a) an odd mode launching condition at a 180° -phase difference, and (b) an even mode launching condition at no phase difference. In Fig. 5(a), the launched longitudinal electric field disappears at the end of the curved region. It is converted to the horizontal electric field (E_y) and focused into the gap region. Figure 5(c) shows the power distribution at the gap region. The light is focused into the gap region. On the other hand, for the even mode launching condition in Fig. 5(b), the launched longitudinal electric field is concentrated at the end of the curved directional coupler region. However, it is not focused into the gap region because of the lack of mode conversion effect, as shown in Fig. 5(d).

longitudinal electric field (E_z) is converted to the horizontal electric field (E_y) and is focused at the gap region. Figure 5(c) shows the propagating power distribution ($|P_{prop}|$) of the gap region. The power intensity is highly focused at the gap region, which proves the mode conversion effect and nanofocusing phenomenon. On the other hand, for the even mode launching in Fig. 5(b), the longitudinal electric field distribution is concentrated at the end of the curved directional coupler region. However, in this case, the mode conversion effect does not occur, and the longitudinal electric field cannot penetrate the gap region due to the mode mismatch. Therefore, as shown in Fig. 5(d), the power distribution is not focused at the gap region.

6. Discussion

The mode conversion effect in the plasmonic directional coupler can be viewed as follows. When the spacing (s) decreases in Fig. 1, the plasmon mode generated by the two metal strips is strongly affected by four corner wedge plasmons in the gap region rather than the surface plasmon mode along the longitudinal metal strip planes (IMI configuration). Therefore, the surface plasmon mode between the two metal strips can be seen as a metal-insulator-metal (MIM) waveguide configuration, where the dispersion equation for the symmetric MIM plasmon mode [26] is:

$$\epsilon_1 k_{y2} + \epsilon_2 k_{y1} \cot\left(\frac{-i k_{y1} d}{2}\right) = 0 \quad (2)$$

$$k_{y1,2}^2 = \epsilon_{1,2} \left(\frac{\omega}{c}\right)^2 - k_y^2 \quad (3)$$

where, $\epsilon_{1,2}$ stands for complex dielectric constants, d is the insulator width, and k_y is the in-plane wave vector.

Any imperfections or asymmetry due to the fabrication process errors in the directional coupler in the regions of (a) and (b) in Fig. 1 causes a phase difference between two waveguides. The phase difference causes even mode generation and it means the reduction of the converged power in the gap region. With an 180° (π) phase change due to imperfection/asymmetry, the odd mode becomes an even mode and no focusing occurs. The actual imperfection/asymmetry length for the odd mode to even mode transition is

$$\left(\frac{\text{Wavelength}}{\text{Effective Index of the strip plasmon mode}}\right) / 2 \quad (4)$$

$$\left(\frac{1.55 \text{ } \mu\text{m}}{2.45}\right) / 2 = \sim 316 \text{ nm} \quad (5)$$

Therefore, the focusing becomes zero with every propagation distance mismatch of 316nm.

To avoid the zero focusing due to fabrication imperfections, one can launch a light only one waveguide in the directional coupler. The fundamental mode in the one waveguide diverges to even and odd modes with a 50:50 power ratio in the coupling region (b) in Fig. 1. As a result, 50 percent of the launched light converges into the gap region as the odd mode if there are no imperfections in the coupling region. The total propagation length of the coupling region is about 700 ~1400 nm and about 300 nm of the propagation distance mismatch is impractical in the whole coupling region.

7. Conclusion

We proposed an efficient nanofocusing method in a gap plasmon waveguide using a mode conversion effect in a strip plasmonic directional coupler. Unlike previous nanofocusing research, we introduced surface plasmon waveguide mode characteristics for nanofocusing at the gap region. The mode characteristics approach has several advantages. First, the waveguide mode basically has a three-dimensional distribution. Therefore, light can converge three-dimensionally at the gap region by decreasing the two-dimensional gap spacing. This means three-dimensional nanofocusing devices can be fabricated with simple conventional semiconductor process. Second, in the directional coupler, most of the light power is carried by the strip plasmon waveguide mode. The imaginary part of the effective index of the strip plasmon waveguide is 0.0224i, whereas that of the gap plasmon waveguide with a 5 nm gap is 0.058349i. Therefore, the absorption loss of the waveguide can be maintained in a relatively low state. Third, the strip plasmon waveguide mode can be launched by external

light sources via evanescent wave coupling with the silicon waveguide. Optical fibers also can be coupled with single metal layer plasmon waveguide configuration at low coupling loss [27]. Fourth, previous nanofocusing simulation research works show higher focusing power and electric field enhancement rates than this mode conversion technique. However, our approach already maintains the three-dimensional additional loss term and propagation loss of the strip plasmon waveguide which are inevitable for the realization of the device. Also, the electric field enhancement rate is compared to that of the strip plasmon waveguide mode which is already amplified its electric field intensity at the metal strip edges. We believe this efficient nanofocusing method will greatly improve research and development in a variety of nano-scale photonic applications.

Acknowledgments

This research was supported by Inha University and by the MSIP (Ministry of Science, ICT & Future Planning), Korea, under the ITRC (Information Technology Research Center) support program (NIPA-2013-H0301-13-1010) supervised by the NIPA (National IT Industry Promotion Agency).